

The Effectiveness of Groin Modifications to Reduce the Impacts of Indian Ocean Dipole (IOD)-induced Port Siltation in Adapting to Climate Change

Andhy Romdani^{1*}, Fahmi Rahmat Amanulloh¹, Mudatsir², Muhammad Raka El Ghifari¹, Zakwan Gusnadi¹, Tryantini Sundi Putri³, Empung¹, Mohammad Syarif Al-Huseiny¹

¹Department of Civil Engineering, Faculty of Engineering, Siliwangi University, Tasikmalaya, INDONESIA

²Department of Medical, Faculty of Medical and Health, Muhammadiyah University of Jakarta, INDONESIA

³Department of Civil Engineering, Faculty of Engineering, Halu Oleo University, Kendari, INDONESIA

*Corresponding author: andhyromdani@unsil.ac.id

SUBMITTED 8 July 2024 REVISED 19 December 2024 ACCEPTED 19 December 2024

ABSTRACT Climate anomalies significantly affect coastal hydrodynamics, influencing sediment transport processes. The interaction between waves and currents plays an important role in sediment transport, which is closely related to climate anomalies, particularly the Indian Ocean Dipole (IOD). Indonesia is currently facing severe threats from port siltation due to the impacts of climate change. Port siltation results from sediment transport and can reduce the effectiveness and safety of port activities. This study aims to investigate sediment transport processes at Titan Coal Port under the influence of the IOD in 2016 and 2019. This port is located on the western coast of Sumatera, where high waves from the Indian Ocean pose a risk. Groins and a breakwater have been installed to protect the port from littoral drift induced by southeastern longshore currents and waves. However, the study found that during the negative IOD in 2016, hydrodynamic conditions led to shallowing of the port basin and navigation channel due to longshore currents from the northeast. The methods used in this research include descriptive analysis (using ERA-5 data from the Copernicus Climate Change Service) and numerical modeling (using MIKE 21) with bed level change identification at several points after groin modification scenarios. The combination of tidal currents and waves primarily shaped current patterns in the study area. High-speed currents caused significant erosion upstream at the bed level of the port basin. However, modified groin installations effectively reduced flow velocity entering the port basin. Two modified groin installation scenarios were tested in the study area to alter existing coastal hydrodynamics and sediment transport patterns.

KEYWORDS climate change, Indian Ocean Dipole (IOD), coal port, sediment transport, port siltation, sedimentation

© The Author(s) 2025. This article is distributed under a Creative Commons Attribution-ShareAlike 4.0 International license.

1 INTRODUCTION

Maritime transportation is the foundation of international trade and the global economy (United Nations Conference on Trade and Development, 2021). According to data from the World Bank and S&P Global Market Intelligence (2023), maritime transportation accounts for 80% of global trade (Humphreys, 2023). The efficiency of maritime transportation determines the effectiveness of shipping activities, particularly in transporting large volumes of cargo. Due to its critical significance, maritime transportation must comply with security and safety regulations.

Seaports significantly support maritime transportation and contribute to a country's economic growth through national and international trade, thereby improving the social standard of communities (Jouili and Allouche, 2016; Munim and Schramm, 2018). High-quality port infrastructure with an effective service system is a key component in enhancing the role of ports in international economic activity. On a global scale, the World Economic Forum (2019) revealed that the quality of port infrastructure in Indonesia ranked 64th with an index of 4.3 (scale 7.0), which is significantly lower than

Singapore, which topped the ranking with an index of 6.5. The challenge of developing ports is the vulnerability of their structure to coastal hazards exacerbated by climate change due to their coastal location (Abdelhafez et al., 2021; Mclean and Becker, 2021). Izaguirre et al. (2021) projected that by 2100, 2,013 ports in the Pacific Islands, Caribbean Sea, and Indian Ocean will be exposed and vulnerable to coastal hazards linked to climate change. Since hydrodynamic conditions and sediment transport patterns along the coast impact seaports, an efficient port management system is necessary to mitigate risks, particularly those related to siltation issues. This aligns with the goals of developing resilient infrastructure and innovation as outlined in the 9th Sustainable Development Goal (SDG) to ensure the adaptation of ports to environmental challenges. Thus, addressing climate change-related port siltation aligns with the 13th SDG goal of promoting climate resilience and proactive adaptation strategies to mitigate the impact of coastal changes (United Nations, 2024).

Excessive sedimentation in the port basin and navigation channel results from natural factors such as geo-

graphic location, bathymetric conditions, the intensity of sea-river currents, riverine sediment input, and climate change patterns (Portillo Juan et al., 2022; Wang and Andutta, 2013). The total sediment load accumulating in the port basin, exceeding the planned capacity, may obstruct ship maneuvers. Severe sedimentation can also cause ships to run aground, disrupting port operations.

Dredging and groin installation are commonly used to manage sedimentation in port basins and navigation channels. The choice of technique begins with the investigation of environmental data such as waves and tidal currents, sediment characteristics, silt concentration, and siltation patterns at the site (Bianchini et al., 2019; Wardani and Murakami, 2019). Dredging is the most popular and reliable method for removing excess sediment to manage port siltation. However, the dredging procedure is inefficient in shallow waters since the costs are higher than in deep waters (van Rijn, 2016). As an alternative, groins help reduce coastal erosion and capture sediment particles before they enter port basins and navigation channels. However, groin installation can be destructive to coastal ecosystems by disrupting the natural sediment flow along the coast. Additionally, maintaining groins is costly due to constant exposure to waves, currents, and saltwater.

Erosion and sedimentation are key coastal hydrodynamics and sediment transport phenomena that researchers and governments have long studied. Many studies have advanced the understanding of these processes through experimental studies and numerical simulations (Afentoulis et al., 2022; Wang and Andutta, 2013). However, understanding sediment transport processes in coastal areas remains incomplete due to the many parameters involved. Climate variability is one of the most dynamic factors influencing sediment transport, particularly under climate change, yet its effects on coastal areas remain underexplored. Climate change alters atmospheric conditions and ocean dynamics, resulting in increased coastal erosion and shoreline shifts (Dong et al., 2024). For instance, in certain Asian coastal areas, a 30 cm rise in sea level can cause up to 45 m of landward erosion (IPCC, 2007). In Indonesia, climate change has intensified coastal erosion, as seen in the Sayung coastal area, Demak Regency, Central Java, where erosion has reached up to 5 km landward (Marfai, 2012).

El Niño-Southern Oscillation (ENSO) and Indian Ocean Dipole (IOD) are two key climate phenomena that have gained increased attention. These climate patterns involve significant variations in sea surface temperature (SST) in the Pacific and Indian Oceans, respectively. Climate change affects coastal hydrodynamics and sediment transport, especially near seaports. Since the study area is in Bengkulu, on the West Coast of Sumatera, which faces the Indian Ocean, IOD likely has

a greater influence than ENSO. This study aims to assess the influence of climate change drivers, particularly IOD, on sediment transport in ports directly exposed to open-sea conditions. Furthermore, solutions for port basin shallowing were explored by evaluating various groin construction strategies

The climate patterns of the Indian Ocean are primarily governed by the annual Asian-Australian Monsoon but can also be influenced by anomalies such as fluctuations in the IOD. The IOD is characterized by significant differences in SST between the western tropical Indian Ocean (WTIO) at 50°E–70°E, 10°S–10°N and the southeastern tropical Indian Ocean (SETIO) at 90°E–110°E, 10°S–0° (Zhang et al., 2018). The IOD is classified based on the Dipole Mode Index (DMI), with values below -1°C indicating a negative phase, neutral conditions in between, and values above $+1^{\circ}\text{C}$ indicating a positive phase. A positive IOD is marked by warmer SST in WTIO and cooler SST in SETIO compared to normal conditions. As a result, atmospheric pressure increases around the western coastal areas of Sumatera Island, causing dominant westward winds. This wind pattern pushes moisture away, leading to drought across most of Indonesia. Conversely, during a negative IOD, warmer SST at SETIO lowers atmospheric pressure, pulling in wind-driven rainfall from the Indian Ocean, leading to increased precipitation across Indonesia.

A strong positive IOD event was recorded in 2019, while a strong negative IOD occurred in 2016 (see Figure 1a). Both extreme IOD phases influence not only Indonesia's climate but also the hydrodynamic behavior of coastal areas, particularly around the Titan Coal Port (see Figure 2a). During extreme IOD phases, strong winds generate high-energy waves, intensifying coastal erosion. Additionally, powerful currents transport sediment loads, increasing sedimentation risks in port basins and navigation channels.

This study compares the impacts of the negative extreme Indian Ocean Dipole (IOD) in the 2016 boreal summer (between June and August) and positive extreme IOD in the 2019 boreal autumn (between September and November) on sedimentation rates at Titan Coal Port, located in the western coastal area of Sumatera, Indonesia. The dominant parameters influencing hydrodynamic processes and sediment transport are then examined. MIKE 21 software was used to investigate the flow pattern changes due to modified groin scenarios aimed at protecting the port basin from the risk of siltation

In this study, the description of the study site is provided in Section 2. The methods and supporting data are explained in Section 3. The analysis of results and discussion are presented in Section 4. The paper concludes with Section 5.

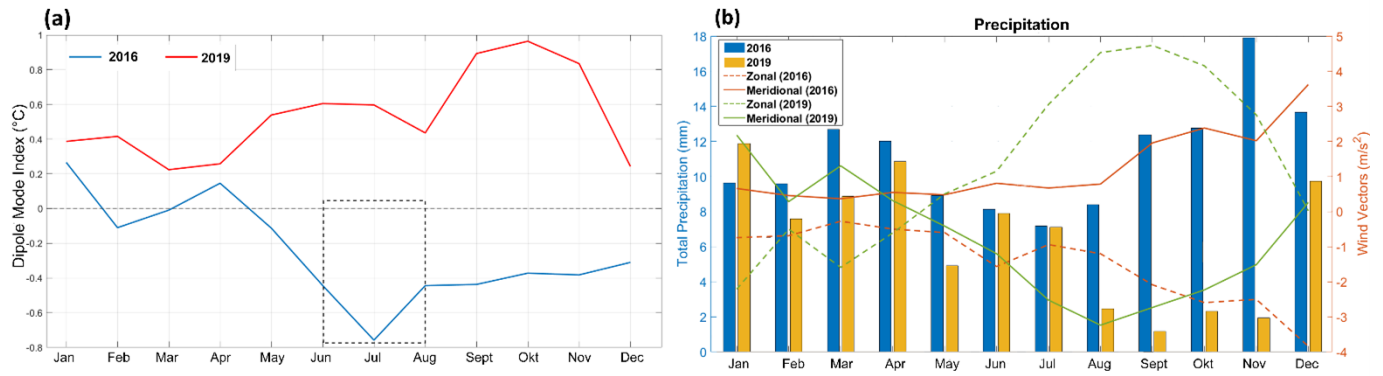


Figure 1 Determination of the simulation period and precipitation intensity: (a). Dipole Mode Index in 2016 (blue line) and 2019 (red line). The dashed box indicates the negative IOD extreme in the 2016 boreal summer; (b). The correlation graph of monthly precipitation fluctuations (2016 is in blue bars and 2019 is in yellow bars) and wind components (zonal wind in dashed line, and meridional wind in solid line) in the study area

2 STUDY AREA

Titan Coal Port is located on the coast of North Bengkulu, at coordinates $-3.285005^{\circ}\text{S}$, $101.672500^{\circ}\text{E}$ (see Figure 2a). This port was constructed to accommodate the 113 km-long coal transportation route that passes through 52 villages, 11 sub-districts, and 4 districts, facilitating the distribution of coal from mines in the South Sumatera region, particularly Muara Enim, Lahat, and Pali. This 14.82-hectare port has a breakwater structure approximately 325 meters long and 454 meters parallel to the coast. The breakwater is designed to prevent sediment loads from being transported into the port basin by southeasterly currents. In addition, the breakwater also serves to block waves from offshore, reducing wave oscillation effects and ensuring safe coal loading operations. Furthermore, this port features a 50-meter-long groin extending perpendicular to the coastline at the mouth of the port, designed to

mitigate sediment loads carried by longshore currents from the northwest. However, due to its direct exposure to the Indian Ocean, Titan Coal Port is highly susceptible to extreme storm effects caused by global climate change

3 METHODS

The methodology used in this study combines descriptive analysis and numerical simulation. The IOD event is observed by visualizing oceanographic data such as SST, wind velocity, total precipitation, and significant wave height (see Table 1 for the parameter data used in the simulation). These data were obtained from the reanalysis dataset ERA-5 of the Copernicus Climate Change Service for the 2016 boreal summer and 2019 boreal autumn. These two periods were selected based on the DMI value from the National Oceanic and Atmospheric Administration (NOAA) to characterize the positive and negative IOD events (see Figure 1a).

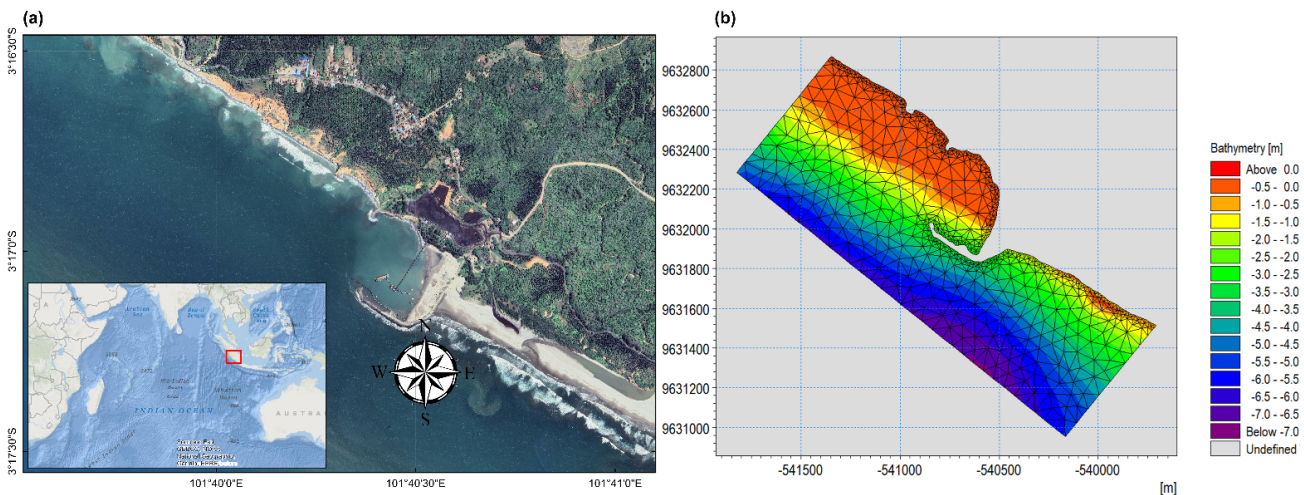


Figure 2 Illustration of the study area and the computational mesh used in the numerical simulation: (a). Map of study area at the coordinates $-3.285005^{\circ}\text{S}$, $101.672500^{\circ}\text{E}$ (source: Esri, Maxar, Earthstar Geographics, and the GIS User Community); (b). 2D mesh of the study area, where bathymetry is represented with contour shading, and grid density differences are shown as gray triangular grids.

Table 1. Parameter data used in the simulation

No.	Parameter	Source	Resolution
1	Sea Surface Temperature	ERA5 Reanalysis	0.25° × 0.25°
2	Wind		0.25° × 0.25°
3	Significant Wave Height		0.5° × 0.5°
4	Bathymetry	BATNAS	6 arc-second

The sediment transport process was investigated through numerical simulations using the MIKE21 software, which accounts for hydrodynamic conditions resulting from different scenarios of modified groin installation. This software provides a dynamic modeling system for applications in coastal, estuarine, and river environments (DHI, 2021). The simulation was conducted to observe changes in the bed level due to the sediment transport process in the port basin under existing conditions and after groin modifications. Satellite images from Google Earth, along with topographic and bathymetric data (obtained from BATNAS, National Bathymetry, Badan Informasi Geospasial (2024)), were used as input for MIKE21 to construct a 2D mesh of the simulation area under both existing and modified conditions (see Figure 2b). Several parameters were used in the simulation, such as wind, tides, waves, and sediment data. Time-series wind data, including wind speed and direction, were incorporated into the simulation. For boundary conditions, tidal data were applied as time series, while wave parameters were set as constant values: a significant wave height of 1 m, a peak wave period of 6 s, and a mean wave direction of 315°. The sediment properties were defined as follows: porosity of 0.4 and grain coefficient of 1.1 (default values), with a relative density of 2.65 and grain size of 0.125 mm, based on laboratory results from a study on coastal abrasion modeling in Pulau Baai Port, Bengkulu (Irmawan et al., 2024).

3.1 Model Scenarios

Some scenarios were conducted to observe the effects of groin modifications on the rate of non-cohesive sediment transport (sand). As a non-cohesive sediment, sand lacks resistance to erosion due to the absence of interparticle bonding. The sand transport module was used to quantify sand transport capacity under the influence of waves and currents (DHI, 2022). The hydrodynamic conditions of the existing groin were simulated to investigate wave and current patterns during the negative IOD event over three months (June to August 2016). Subsequently, two modified groin scenarios were simulated to evaluate their effectiveness in reducing sedimentation levels in the port basin. To assess the impact of waves on hydrodynamic processes in the study area, wave parameters were incorporated as

wave radiation stress. The time-series boundary conditions (northwest, southwest, and southeast) were derived from predicted tidal parameters.

The calibration process of the coastal hydrodynamics model was carried out using tidal data obtained from a tide monitoring station in Padang. A total of 43,197 data points were recorded as a time series with one-minute intervals from June 1, 2016, at 00:00 to July 1, 2016, at 00:00. Figure 3 shows the surface elevation calibration results, comparing observational data and model outputs, with a root mean square error (RMSE) value of 0.0830, indicating good model performance.

To ensure model stability, the minimum and maximum internal time steps were set at 0.01 s and 3600 s, respectively, with a CFL adjustment number of 0.9. The Coriolis force was incorporated into the simulation with a variable coefficient across the domain. The model was configured with an eddy viscosity of 0.28 m²/s (Smagorinsky formulation) and a Manning's number of 32 m^(1/3)/s for open water (Boyden et al., 2021; DHI Water & Environment, 2006). These values are essential for understanding the impact of wave-induced currents on bed level changes.

3.2 Model Equations

The accuracy and performance of various models, including silt transport and spectral waves, are significantly influenced by the hydrodynamic conditions simulated using MIKE 21. This model captures the dynamic behavior of water levels and flows in response to external forces. It solves the incompressible Reynolds-averaged Navier-Stokes equations under the Boussinesq and hydrostatic pressure assumptions, utilizing the continuity equation and two horizontal momentum equations for the x and y components. The depth-integrated continuity equation is given as:

Continuity equation

$$\frac{\partial h}{\partial t} + \frac{\partial h\bar{u}}{\partial x} + \frac{\partial h\bar{v}}{\partial y} = hS \quad (1)$$

The horizontal momentum equation for the x -component

$$\begin{aligned} \frac{\partial h\bar{u}}{\partial t} + \frac{\partial h\bar{u}^2}{\partial x} + \frac{\partial h\bar{u}\bar{v}}{\partial y} = & fh\bar{v} - gh\frac{\partial\eta}{\partial x} - \frac{h}{\rho_0}\frac{\partial P_a}{\partial x} - \frac{gh^2}{2\rho_0}\frac{\partial\rho}{\partial x} \\ & + \frac{\tau_{sx}}{\rho_0} - \frac{\tau_{bx}}{\rho_0} - \frac{1}{\rho_0}\left(\frac{\partial S_{xx}}{\partial x} + \frac{\partial S_{xy}}{\partial y}\right) \\ & + \frac{\partial}{\partial x}hT_{xx} + \frac{\partial}{\partial y}HT_{xy} + hu_sS \end{aligned} \quad (2)$$

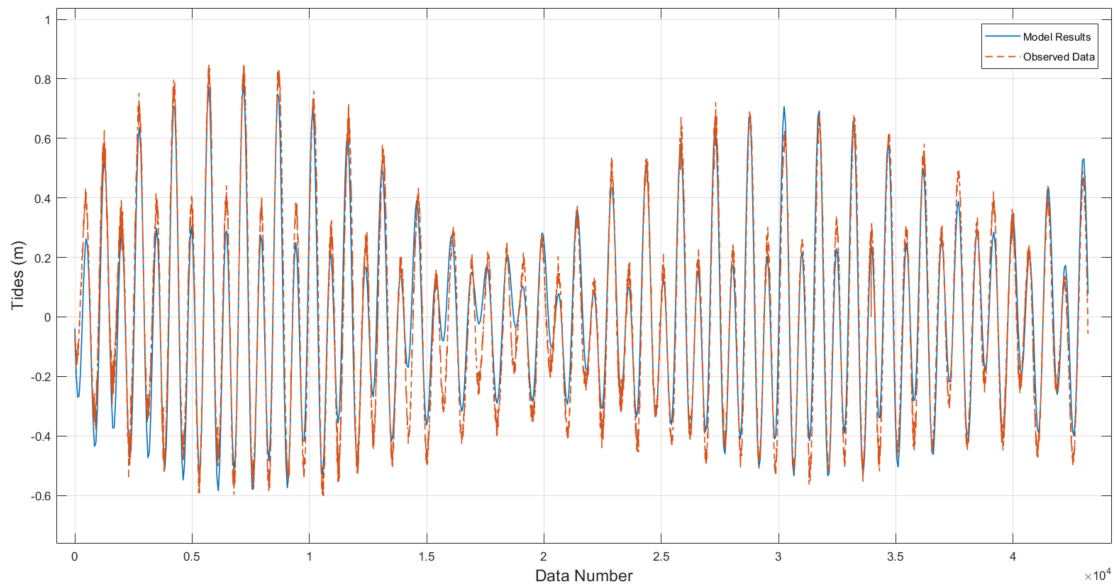


Figure 3 Calibration result between modeled and observed data.

The horizontal momentum equation for the y -component

$$\begin{aligned} \frac{\partial h\bar{u}}{\partial t} + \frac{\partial h\bar{v}\bar{u}}{\partial x} + \frac{\partial h\bar{v}^2}{\partial y} = & fh\bar{u} - gh\frac{\partial\eta}{\partial y} - \frac{h}{\rho_0}\frac{\partial P_a}{\partial y} - \frac{gh^2}{2\rho_0}\frac{\partial\rho}{\partial y} \\ & + \frac{\tau_{sy}}{\rho_0} - \frac{\tau_{by}}{\rho_0} - \frac{1}{\rho_0}\left(\frac{\partial S_{yx}}{\partial x} + \frac{\partial S_{yy}}{\partial y}\right) \\ & + \frac{\partial}{\partial y}hT_{xy} + \frac{\partial}{\partial y}HT_{yy} + hv_sS \end{aligned} \quad (3)$$

where x and y are the Cartesian coordinates; g is gravity acceleration; t is time; \bar{u} and \bar{v} are the averaged velocity components in the x and y directions, respectively; $h = \eta + d$ is the total water depth; η is the water surface elevation; d is the still water depth; f is the coefficient of the Coriolis force; $f_{\bar{u}}$ and $f_{\bar{v}}$ are accelerations caused by the rotation of the Earth; P_a is the air pressure; ρ_0 is the normal seawater density; ρ is the density of water; $\tau_{xx}, \tau_{xy}, \tau_{yy}$ are the horizontal viscous stress terms; $S_{xx}, S_{xy}, S_{yx}, S_{yy}$ are the wave radiation stress; S is the source and sink item; u_s and v_s are the flow rates of the head and sink flows.

Sediment transport

Modeling sediment transport involves complex interactions between hydrodynamic forces and sediment behavior. Since sediment transport modeling relies on empirical formulations, experimental data and calibration parameters are used to refine the model. To simplify the modeling process, sediment transport is divided into two modes: bed load and suspended load. The total sediment transport is given by:

$$q_t = q_b + q_s \quad (4)$$

where q_t is the total sediment transport; q_b is the bed load transport induced by shear stress on the seabed; and q_s is the sediment transport in suspension due to wave, sediment concentration, and shear stress on the seabed.

Control equation of sediment transport model:

$$\begin{aligned} \frac{\partial\bar{c}}{\partial t} + u\frac{\partial\bar{c}}{\partial x} + v\frac{\partial\bar{c}}{\partial y} = & \frac{1}{h}\frac{\partial}{\partial x}\left(hD_x\frac{\partial\bar{c}}{\partial x}\right) + \frac{1}{h}\frac{\partial}{\partial y}\left(hD_y\frac{\partial\bar{c}}{\partial y}\right) \\ & + Q_L C_L \frac{1}{h} - S \end{aligned} \quad (5)$$

where \bar{c} is the average sediment concentration in the water depth direction (kg/m^3); D_x and D_y are the dispersion coefficients in the x and y directions; Q_L is the source discharge divided by area ($\text{m}^3/(\text{sm}^2)$); C_L is the source sediment concentration (kg/m^3); and S is the scouring/silting item (m^2/s).

The settling speed of sediments is calculated using the Stokes' settling velocity formula:

$$\omega = \frac{(\rho_s - \rho)gd_s^2}{18\rho\nu} \quad (6)$$

where ω is the sedimentation velocity (m/s); ρ_s is the bulk density of the sediment (kg/m^3); ρ is the bulk density of water (kg/m^3); g is the acceleration of gravity

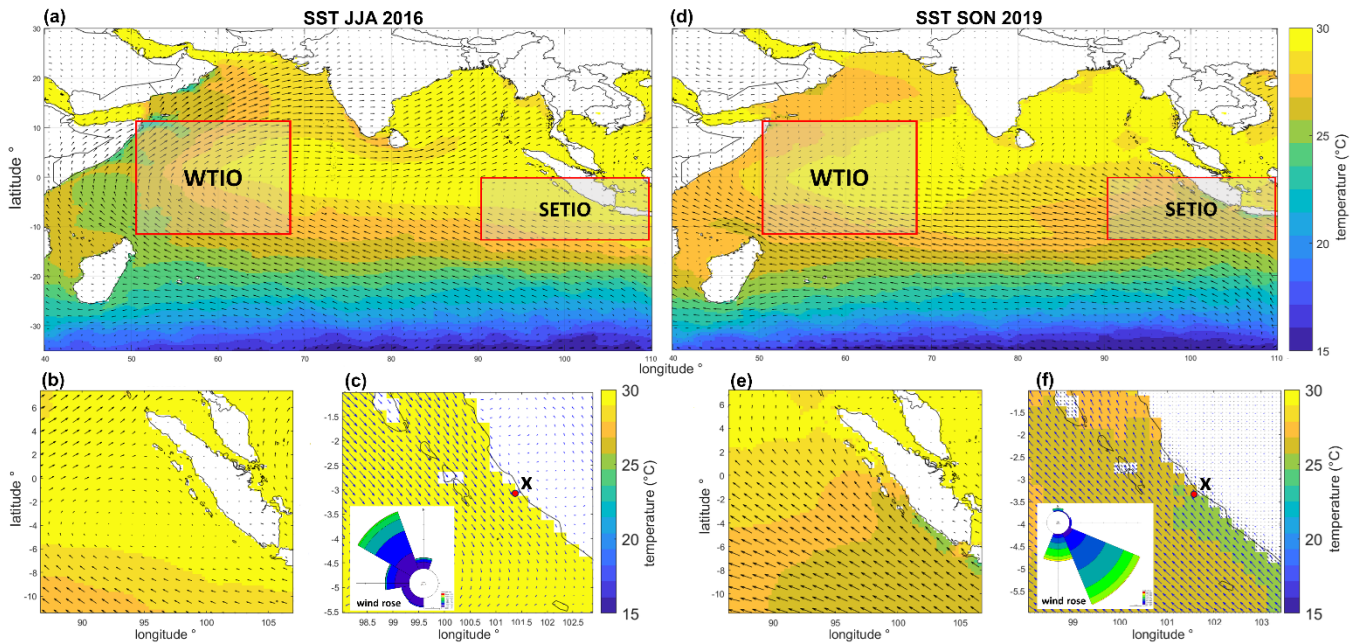


Figure 4 Sea surface temperature (SST) and wind patterns during the JJA 2016 and SON 2019: (a). The anomaly of SST (in contour shading, unit °C) and wind circulation (in black vectors, unit m/s) during 2016 boreal summer; (b). Wind circulation around Sumatera Island (in black vectors); (c). Northwestly wind in the study area; (d). The anomaly of SST (in contour shading, unit °C) and wind circulation (in black vectors, unit m/s) during 2019 boreal autumn; (e). Wind circulation around Sumatera Island (in black vectors); (f). Southeastern wind in the study area.

(m/s^2); d_s is the sediment particle size (m); and ν is the kinematic viscosity coefficient of the water flow (m^2/s).

4 RESULTS AND DISCUSSION

4.1 Anomaly of Sea Surface Temperature (SST) and Wind Patterns

SST conditions at the WTIO and SETIO are the main factors in forming wind circulation in the Indian Ocean region. The interaction between the ocean and atmosphere causes different atmospheric pressures, determining the wind direction and speed. High SST induces atmospheric pressure to decrease, while low SST causes pressure to increase. Figure 4a shows a higher SST of approximately 28.82 °C–29.82 °C in the eastern Indian Ocean, including the SETIO region, in the 2016 boreal summer. Meanwhile, the SST in the WTIO region has a lower temperature of 28.57 °C, resulting in higher atmospheric pressure compared to the SETIO area. Wind movement starts from the southern region of the Indian Ocean towards the western Indian Ocean in the WTIO region, then it turns at the equator line towards the east due to the influence of the Coriolis effect. Subsequently, the wind flows towards the coastal areas of western Indonesia, which directly affects the study area on the coast of Sumatera (Figure 4b). This phenomenon, known as the negative IOD, has the potential to increase rainfall intensity in Indonesia, particularly on Sumatera Island. Extreme negative IOD also strengthens wind-induced currents from the

northwest direction to the west coast of Sumatera (see Figure 4c). Longshore currents carrying sediment loads due to strong winds from the northwest direction could potentially reach the port basin, causing siltation.

The positive IOD in the 2019 boreal autumn in Figure 4d demonstrates the decline of SST in the SETIO region of approximately 26.98 °C, lower than those in the WTIO region of 29.6 °C. The dominant winds with a mean velocity of 4.48 m/s from the southeast stretched along the coastline of western Sumatera (Figure 4e). Wind movement from the southeast is not a phenomenon that should be of concern for the siltation of Titan Coal Port on the coast of Bengkulu (Figure 4f). The existing breakwater position was designed to protect against longshore drift under these conditions (see Figure 2a). Even if it does not induce siltation in the port basin, the energy of the longshore current from the southeast can cause changes in the coastline due to accretion in the downdrift area.

4.2 Effects of Precipitation on Hydrodynamic Processes

Rainfall intensity was significantly different between the negative IOD 2016 and the positive IOD 2019 (see Figure 1b). The IOD phenomenon greatly impacts the intensity of rainfall in the 2016 boreal autumn, raising it above normal conditions at the beginning of the rainy season in Indonesia (normally from September to October), but drastically decreasing the rainfall intensity in the 2019 boreal autumn. This anomalous rainfall con-

dition can be explained by the movement of zonal and meridional winds in Figure 1b. In 2016, zonal winds (red dashed line) were consistently in a negative direction (east–west), while meridional winds (red solid line) were in a positive direction (north–south). Both zonal and meridional winds began to increase, resulting in high rainfall from September to November. Conversely, in 2019, zonal winds were in a positive direction (west–east), while meridional winds were in a negative direction (south–north). This wind condition resulted in low rainfall intensity, with the peak occurring in SON 2019 when zonal and meridional winds reached maximum speed in the positive and negative directions, respectively.

According to the DMI in Figure 1a, the 2019 boreal autumn was the highest index during 2019, which also caused a drastic decrease in rainfall intensity in the same period (see Figure 1b, SON 2019). On the other hand, the 2016 boreal summer was also the lowest in-

dex during 2016. However, the highest level of precipitation occurred in the 2016 boreal autumn, which is not in line with the minimum index value (see Figure 1a, JJA 2016, and Figure 1b, JJA 2016). Based on this anomaly, it can be assumed that an IOD index can serve as a guide for characterizing IOD phenomena (positive or negative), but it cannot be used to determine low or high precipitation amounts. High levels of precipitation at negative IOD or low levels of precipitation at positive IOD are simply a side effect of the influence of the IOD phenomenon on wind circulation. By considering the IOD index and dominant wind direction, the 2016 boreal summer was simulated to determine the dominant parameters in hydrodynamic processes and sediment transport.

Figure 5a shows the hydrodynamic conditions in the study area due to the influence of precipitation on current speed. When precipitation began to increase (see Figure 5c, green box), the current speed became lower

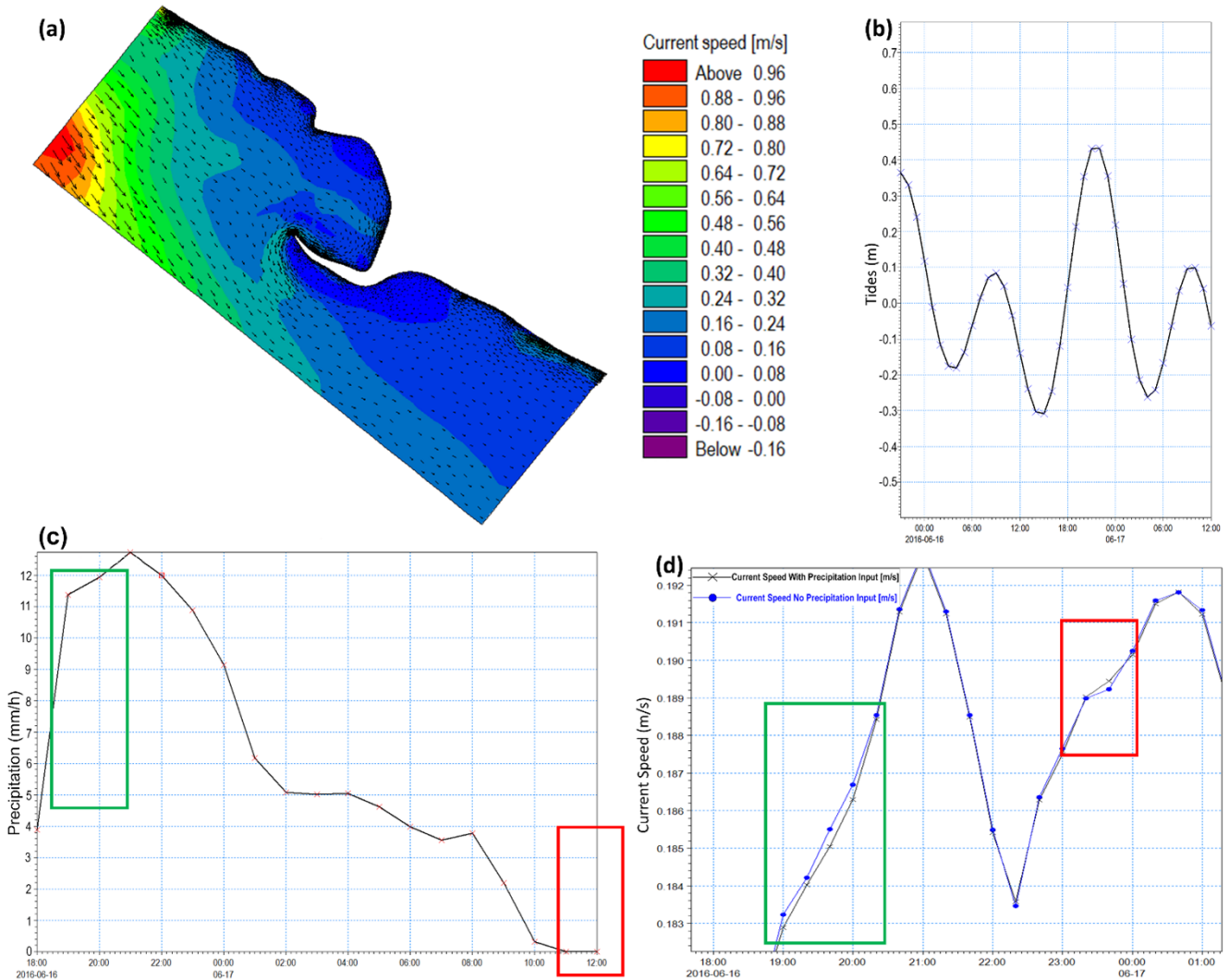


Figure 5 The influence of precipitation on hydrodynamic processes: (a) The modeled result showing current speed during peak precipitation in 17 June 2016 at 9.00 a.m.; (b) Tidal fluctuations (from 6/15/2016 at 9:00:00 p.m. to 6/17/2016 at 12:00:00 p.m.); (c) Rainfall intensity; (d) Comparison of the current speed between the simulations with and without precipitation.

(see Figure 5d, black line) compared to modeling results without precipitation input (blue line). On the other hand, when precipitation decreased (Figure 5c, red box), the flow velocity increased (Figure 5d, red box) compared to the flow model without precipitation input. This is likely due to the influence of precipitation, which slows down the current circulation in the study area.

Both simulations with and without precipitation utilize the same input tidal data (Figure 5b) and wind. The simulated results demonstrate insignificant differences even during the highest intensity of precipitation events. Although the IOD phenomenon is closely related to the increase and decrease in rainfall, it does not directly affect coastal hydrodynamic conditions. In general, changes in rainfall intensity are a side effect of wind movement patterns due to pressure differences. Furthermore, the wind-generated wave and tidal movement patterns due to the IOD phenomenon were investigated for their influence on the hydrodynamic conditions in the study area.

4.3 Coastal Hydrodynamics Influenced by Waves and Currents

Wind-generated waves and tides are parameters that form hydrodynamic patterns in coastal areas, which influence sediment transport processes induced by currents. In general, the dominant winds formed in the

study area move from the northwest during negative IOD 2016 and blow from the southeast during positive IOD 2019 (see Figure 4). These two phenomena form different wind-generated waves in the study area and generate longshore currents. The condition of the existing Coal Port Titan with a 50 m groin makes it exposed to longshore currents in the northwest direction, which poses a risk of accelerating shallowing in the port basin (see Figure 6a).

The risk of siltation in the existing port basin can be mitigated by modifying the current circulation pattern, through modifications to the shape, dimension, and location of the groin. Figure 6 shows changes in flow patterns and velocities due to the presence of the existing groin. In general, the installation of a groin changes the current patterns around the port. Modified groin 1 (Figure 6b) involves extending the existing groin to 200 m with the addition of a bent groin at the end extending 70 m. This modification aims to change the direction of longshore currents from the northwest, diverting sediment away from the port basin. Modified groin 2 (Figure 6c) was used to block longshore drift. This scenario involves extending the existing groin to 200 m with the addition of two groins on the upstream side, each measuring 130 m and 125 m long, perpendicular to the coastline. The effectiveness of the groin installations can be seen through the current speed at the mouth of the port (t1) at coordinates -540843.22 m, and 9632129.77 m. The simulated results demonstrate

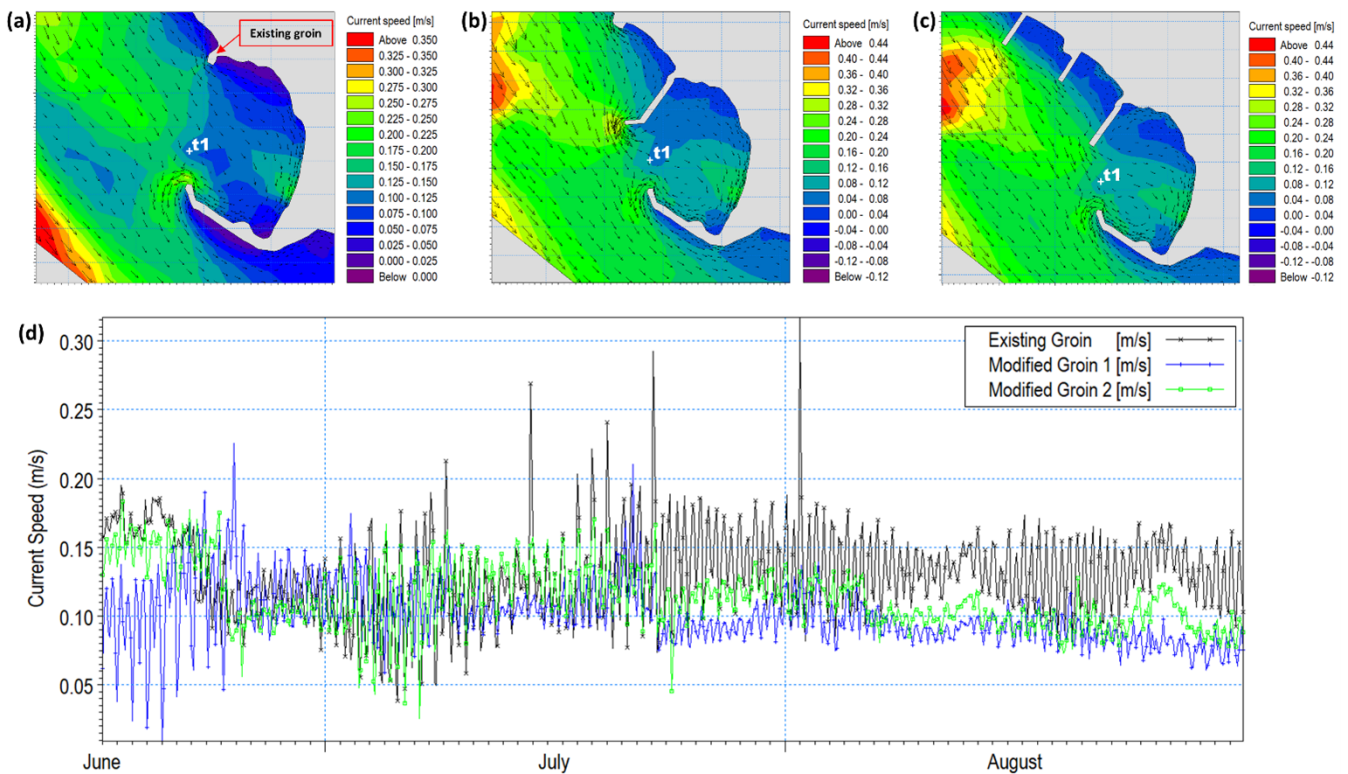


Figure 6 The effects of waves and currents on coastal hydrodynamics due to: (a) Existing groin; (b) modified groin 1; (c) modified groin 2; (d) comparison of current speeds between existing and modified groins.

that the modified groins 1 and 2 were effective in reducing the flow velocity entering the port basin (see Figure 6d).

4.4 Impacts of Groin Installation on Reducing Sedimentation in Port Basin

This section examines the impacts of groin modifications on reducing sedimentation in the basin of Titan Coal Port, Bengkulu, due to the influence of climate change-triggered Indian Ocean Dipole (IOD). The sedimentary process is greatly influenced by the hydrodynamic conditions of the coastal area, which determine the pattern of currents in transporting sediment loads. Apart from wind-generated waves and tides, coastal structure installations such as groin and breakwaters can also change the current patterns in the surrounding area. Figure 7 shows the simulated results of bed level changes due to sediment transport processes in the existing conditions and two scenarios of the modified groin. Three points were used to observe sedimentation patterns in the port basin. Point t1 located at the mouth of the port was examined to observe changes in bed level due to the direct influence of longshore currents from the northwest direction. Point t2 was set in the port basin, chosen to investigate the sedimentation process induced by sediment transfer at point t1. Point t3 was the point where the current circulates and exits the port basin, depicted as the site where sediment loads accumulate from points t1 and t2.

Under existing conditions (Figure 7a), longshore currents caused an increase in bed level at points t1 and t3 (Figure 7d). On the other hand, point t2 experiences erosion due to current-driven sediment transport, leading to point t3. Modified groin 1 (Figure 7b) demon-

strated that the mouth of the port is in a balanced condition (see black line, which is relatively stable on the $y=0$ axis in Figure 7e). The extension of the groin was relatively capable of preventing sediment from entering the port basin due to changes in current patterns at the mouth of the port. Significant differences occurred at points t2 and t3 which experience accretion and erosion, respectively (Figure 7e). In general, modified groin 1 was effective in stabilizing the bed level at the mouth of the port, maintaining the safe entry and exit for vessels. Modified groin 2 (Figure 7c) caused the mouth of the port (point t1) and port basin (point t2) to experience erosion, triggering the siltation point t3 (see Figure 7f). Sediment accumulation at point t3 was an advantage in maintaining the effectiveness of the coal port due to no obstruction to the vessel movements. Moreover, the sediment dredging process will become more accessible.

Sedimentation in the port basin is a complex natural process. However, the choice of groin installation can be made based on its effectiveness in reducing sedimentation levels in the port basin. The simulated results in Figures 7a and 7d depict that the sediment accumulated at the mouth of the port, which has risks of disrupting the vessel movements due to siltation. Groin modification is studied as an alternative option that can be applied to overcome port siltation issues. The mouth of the port and basin areas near the breakwater are the dominant areas for sediment accumulation. The observation was carried out by drawing a straight line from the mouth of the port along the breakwater for 280 m (see Figure 7g, line A-B). The simulated results show that the modified groin 1 has great potential to reduce sedimentation levels. However, at the location between 140–210 m from the mouth of the port, a significant increase in bed level occurred (see

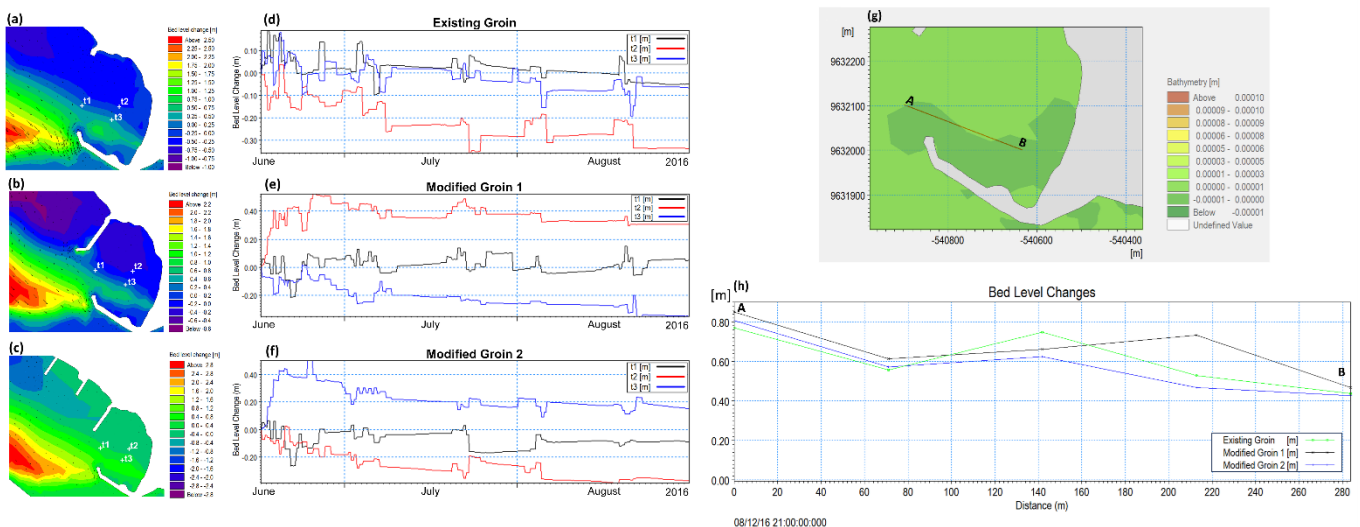


Figure 7 The impacts of groin installation on reducing sedimentation in the port basin: (a) Straight line from the mouth of the port along the breakwater for 280 m to observe the bed level changes; (b) variations of bed level changes; (g) Straight line from the mouth of the port along the breakwater for 280 m to observe the bed level changes; (h) variations of bed level changes.

Figure 7h, black line). On the other hand, a similar pattern occurred between the existing conditions and modified groin 2 with a smaller increase in bed level at up to 80 m. Greater effectiveness in reducing sedimentation levels in the port basin occurred when modified groin 2 was chosen, showing a reduction at 80–280 m with a lower bed level change (see Figure 7h, blue line).

5 CONCLUSION

The hydrodynamic conditions and sediment transport processes near seaports are impacted by climate change. IOD is one indication of climate change that has posed the risk of siltation in Titan Coal Port, Bengkulu, Western Coast of Sumatera. The positive IOD extreme 2019 boreal autumn induced southeasterly wind-driven littoral drift. Fortunately, the existence of a breakwater can protect the port basin from siltation issues. In contrast, the negative IOD extreme 2016 boreal summer caused the dominant winds to move from the Indian Ocean to the coast of Sumatera Island. Consequently, the areas surrounding the Titan Coal Port experienced significant changes triggered by wind-generated waves from the Indian Ocean. North-westerly littoral drift could potentially induce the port siltation.

The mitigation of port siltation can be carried out by modifying the existing groins according to shape, dimension, and location. The simulated results demonstrate that the modified groin 1 (extending the existing groin to 200 m with the addition of a bent groin at the end of 70 m) and groin 2 (extending the existing groin to 200 m with the addition of two groins at the upstream side, each 130 m and 125 m long, perpendicular to the coastline) were effective in reducing the flow velocity entering the port basin. In terms of maintaining the effectiveness of the Titan Coal Port, the modified groin 2 was more effective in slowing the port siltation. The minimum sedimentation levels in the port basin can be found if modified groin 2 is applied in the study area.

DISCLAIMER

The authors declare no conflict of interest.

ACKNOWLEDGMENTS

We want to express our gratitude to the Rector of Siliwangi University, the Dean of the Faculty of Engineering, and the Head of the Department of Civil Engineering for their essential support and contribution to finishing this research.

AUTHOR CONTRIBUTION

AR and FRA contributed to conceptualization, methodology, writing the original draft, and editing the writing. M, MREG, ZG, TSP, E, and MSA contributed to reviewing the writing. FA and MREG contributed to software analyses, data curation, and visualization. AR contributed to supervision. All authors have read and agreed to the published version of the manuscript.

REFERENCES

- Abdelhafez, M. A., Ellingwood, B. and Mahmoud, H. (2021), 'Vulnerability of seaports to hurricanes and sea level rise in a changing climate: A case study for mobile, al', *Coastal Engineering* **167**, 103884.
URL: <https://doi.org/10.1016/j.coastaleng.2021.103884>
- Afentoulis, V., Papadimitriou, A., Belibassakis, K. and Tsoukala, V. (2022), 'A coupled model for sediment transport dynamics and prediction of seabed morphology with application to 1dh/2dh coastal engineering problems', *Oceanologia* **64**(3), 514–534.
URL: <https://doi.org/10.1016/j.oceano.2022.03.007>
- Badan Informasi Geospasial (2024), 'Batnas', Dataset. Retrieved from <https://tanahair.indonesia.go.id/porta-l-web/unduh/batnas>.
- Bianchini, A., Cento, F., Guzzini, A., Pellegrini, M. and Saccani, C. (2019), 'Sediment management in coastal infrastructures: Techno-economic and environmental impact assessment of alternative technologies to dredging', *Journal of Environmental Management* **248**, 109332.
URL: <https://doi.org/10.1016/j.jenvman.2019.109332>
- Boyden, P., Casella, E., Daly, C. and Rovere, A. (2021), 'Hurricane matthew in 2100: Effects of extreme sea level rise scenarios on a highly valued coastal area (palm beach, fl, usa)', *Geo-Marine Letters* **41**(4), 43.
URL: <https://doi.org/10.1007/s00367-021-00715-6>
- DHI (2021), 'Mike flood: Urban, coastal, and riverine flooding'. Retrieved from <https://www.mikepoweredbydhi.com/products/mike-flood>.
- DHI (2022), *MIKE 21 & MIKE 3 Flow Model FM: Sand Transport Module*.
URL: https://manuals.mikepoweredbydhi.help/2019/Coast_and_Sea/MIKE_FM_ST_Scientific_Doc.pdf
- DHI Water & Environment (2006), *MIKE 21 Flow Model: Hydrodynamic Module User Guide*, DHI Water & Environment.
URL: <https://www.dhigroup.com/technologies/mikepoweredbydhi/downloads-and-support>
- Dong, W. S., Ismailluddin, A., Yun, L. S., Ariffin, E. H., Saengsupavanich, C., Abdul Maulud, K. N., Ramli, M. Z.,

Miskon, M. F., Jeofry, M. H., Mohamed, J., Mohd, F. A., Hamzah, S. B. and Yunus, K. (2024), 'The impact of climate change on coastal erosion in southeast asia and the compelling need to establish robust adaptation strategies', *Heliyon* **10**(4), e25609.

URL: <https://doi.org/10.1016/j.heliyon.2024.e25609>

Humphreys, R. M. (2023), 'Why ports matter for the global economy', World Bank Blog.

URL: <https://blogs.worldbank.org/en/transport/why-ports-matter-global-economy>

IPCC (2007), 'Climate change 2007: Impacts, adaptation and vulnerability'.

Irmawan, M., Imaaduddin, M. H., Alam, R. R. R., Refani, A. N. and Aini, A. N. (2024), 'Hydrodynamic analysis-based modeling of coastal abrasion prevention (case study: Pulau baai port, bengkulu)', *Applied Sciences* **14**(2), 940.

URL: <https://doi.org/10.3390/app14020940>

Izaguirre, C., Losada, I. J., Camus, P., Vigh, J. L. and Stenek, V. (2021), 'Climate change risk to global port operations', *Nature Climate Change* **11**(1), 14–20.

URL: <https://doi.org/10.1038/s41558-020-00937-z>

Jouili, T. and Allouche, M. (2016), 'Impacts of seaport investment on the economic growth', *Promet - Traffic - Traffico* **28**, 365–370.

Marfai, M. A. (2012), 'Preliminary assessment of coastal erosion and local community adaptation in sayung coastal area, central java – indonesia', *Quaestiones Geographicae* **31**(3), 47–55.

URL: <https://doi.org/10.2478/v10117-012-0028-2>

McLean, E. L. and Becker, A. (2021), 'Advancing seaport resilience to natural hazards due to climate change: Strategies to overcome decision making barriers', *Frontiers in Sustainability* **2**.

URL: <https://doi.org/10.3389/frsus.2021.673630>

Munim, Z. H. and Schramm, H.-J. (2018), 'The impacts of port infrastructure and logistics performance on economic growth: The mediating role of seaborne trade',

Journal of Shipping and Trade **3**(1), 1.

URL: <https://doi.org/10.1186/s41072-018-0027-0>

Portillo Juan, N., Negro Valdecantos, V. and del Campo, J. M. (2022), 'Review of the impacts of climate change on ports and harbours and their adaptation in Spain', *Sustainability* **14**(12).

URL: <https://doi.org/10.3390/su14127507>

United Nations (2024), 'The 17 goals'.

URL: <https://sdgs.un.org/goals>

United Nations Conference on Trade and Development (2021), *Review of Maritime Transport 2021*, United Nations.

URL: <https://doi.org/10.18356/9789210000970>

van Rijn, L. (2016), 'Harbour siltation and control measures'.

URL: <https://www.leovanrijn-sediment.com/papers/Harboursiltation2012.pdf>

Wang, X. H. and Andutta, F. P. (2013), 'Sediment transport dynamics in ports, estuaries and other coastal environments', in A. J. Manning, ed., 'Sediment Transport Processes and Their Modelling Applications', IntechOpen.

URL: <https://doi.org/10.5772/51022>

Wardani, K. S. and Murakami, K. (2019), 'The effectiveness of groin system on the control of sediment transport', *Journal of Japan Society of Civil Engineers, Ser. B2 (Coastal Engineering)* **75**(2), I₅35 – I₅40.

URL: https://doi.org/10.2208/kaigan.75.I_535

World Economic Forum (2019), 'Port infrastructure quality - country rankings'.

URL: https://www.theglobaleconomy.com/rankings/seaports_quality/

Zhang, L., Du, Y. and Cai, W. (2018), 'Low-frequency variability and the unusual Indian Ocean dipole events in 2015 and 2016', *Geophysical Research Letters* **45**(2), 1040–1048.

URL: <https://doi.org/10.1002/2017GL076003>

[This page is intentionally left blank]